Optical Engineering

OpticalEngineering.SPIEDigitalLibrary.org

Surface inspection system for industrial components based on shape from shading minimization approach

Muhammed Kotan
Cemil Öz

SPIE.

Muhammed Kotan, Cemil Öz, "Surface inspection system for industrial components based on shape from shading minimization approach," *Opt. Eng.* **56**(12), 123105 (2017),
doi: 10.1117/1.OE.56.12.123105.

Surface inspection system for industrial components based on shape from shading minimization approach

Muhammed Kotan[a,*] **and Cemil Öz**[b]
[a]Sakarya University, Department of Information Systems Engineering, Faculty of Computer and Information Sciences, Sakarya, Turkey
[b]Sakarya University, Department of Computer Engineering, Faculty of Computer and Information Sciences, Sakarya, Turkey

Abstract. An inspection system using estimated three-dimensional (3-D) surface characteristics information to detect and classify the faults to increase the quality control on the frequently used industrial components is proposed. Shape from shading (SFS) is one of the basic and classic 3-D shape recovery problems in computer vision. In our application, we developed a system using Frankot and Chellappa SFS method based on the minimization of the selected basis function. First, the specialized image acquisition system captured the images of the component. To eliminate noise, wavelet transform is applied to the taken images. Then, estimated gradients were used to obtain depth and surface profiles. Depth information was used to determine and classify the surface defects. Also, a comparison made with some linearization-based SFS algorithms was discussed. The developed system was applied to real products and the results indicated that using SFS approaches is useful and various types of defects can easily be detected in a short period of time. [DOI: 10.1117/1.OE.56.12.123105]

Keywords: industrial inspection; defect detection; shape from shading; three-dimensional shape recovery.

Paper 171179 received Jul. 27, 2017; accepted for publication Nov. 14, 2017; published online Dec. 12, 2017.

1 Introduction

The quality control in mass production has increased considerably in recent years with computer vision methods. Almost any kind of industry, such as automotive and manufacturing, can benefit from the use of three-dimensional (3-D) imaging. Since some of the produced parts are of very delicate quality and scrapped in the event of a slight physical deformation, automated visual inspection systems have been widely used since the late 1980s, and new various automatic methods for detecting surface have been developed recently.[1,2] To prevent human faults, such as fatigue and absent-mindedness, increase production rate, and be quick in decision-making, it is generally necessary to use computer vision in mass production.

The quality control of a 3-D object in two dimensions through computer vision may contain some difficulties. The acquired images of the components may sometimes be unclear, may be noisy, or the image processing algorithm may be insufficient or show poor performance. It can be difficult to detect a defect in such situations. There are many studies in the literature to detect surface defects of parts, including filters such as Median filter and Gabor filter in gray-level images, using pattern recognition systems, using methods such as decision trees, artificial neural networks, nearest neighbors (1-NN), and support vector machines.[3–7] For a better detection of defects, some surface inspection methods using 3-D reconstruction techniques have also been studied in the literature.[8–10]

The shape of an object can be obtained from its one or more images, and in general, there are many different methods, such as shading, photometric stereo, texture, motion, and shadows under "shape from X" heading (see Fig. 1).[11,12] Shape recovery is a classic problem in computer vision. The goal is to derive a 3-D scene description from one or more two-dimensional (2-D) images. The recovered shape can be expressed as depth, surface normal, surface gradient, and surface angles.[13]

Each method has its own advantages and disadvantages. In particular, stereo and shading methods are extensively being used in the literature for inspection purposes.[10,14,15]

Shape from shading (SFS) is one of the basic and classic 3-D shape recovery problems in computer vision. SFS methods can be classified into three or four approximations based on the technique used to recover 3-D shape.[13,16] We focused on Frankot and Chellappa SFS technique, and estimated depth information was used in the decision-making phase of the inspection system.

The goal of this work is to develop a simple and easy to implement surface inspection system using SFS methods based on function minimization. The image acquisition system captured the images of the component, and the output is converted to digital format. Often the image is first manipulated to reduce noise. First, to reduce the image noise, we used a wavelet smoothing method that has been successful in smoothing applications and reducing the noise very effectively.[17–19] After wavelet filtering, the proposed SFS technique was used to obtain depth and surface profiles. Obtained depth information was used to determine the surface defects.

The remaining parts of this paper are organized as follows. Section 2 explains system illumination, SFS basics and describes the selected Frankot and Chellappa approach. In Sec. 3, we apply the improved algorithm to recover the shape of the product and show how estimated gradients and depth information are used for the purpose of defect

*Address all correspondence to: Muhammed Kotan, E-mail: mkotan@sakarya.edu.tr

detection. Finally, experimental results and future trends in the field are discussed in Sec. 4, followed by conclusions in Sec. 5.

2 System Background

Obtaining depth information of the surfaces with shape recovery methods depends on some factors, such as direction, spectral energy distribution and spatial position of illumination, surface reflectivity, geometry of the surface, projective system, etc. Given the illumination direction, reflectivity, and surface geometry, an image can be rendered to simulate the projective system process. SFS is the inverse problem, given an image, it is required to recover the surface geometry. Surface gradients, surface normals, imperfect light source knowledge, reflectance, albedo variations, and some other parameters make the inverse problem ill-posed. Therefore, researchers have used assumptions about the problem. As SFS has an extensive literature, we refer the readers to Refs. 13 and 16 surveys describing and comparing SFS techniques. There are also recently used some new perspective SFS techniques. Orthographic projection, Lambertian surface, known or estimated illumination directions and constant albedo conditions are often the simplest scenerio for SFS algorithms. The following steps describe the methodologies we use in our system.

2.1 *Illumination Source*

A robust, quality, and timely inspection can be achieved with a properly configured illumination system. Study of illumination techniques, surface geometry, filtering, sensor characteristics, and the performance of the illumination system are all essential for SFS algorithms and machine vision. To easily and accurately detect different surface defects, improve performance, and facilitate the inspection process, special illumination systems are required.

Light-emitting diode (LED) lights are commonly used as the illumination source in machine vision technology and can be used for different types of defects for automatic detection.[20] A sample dome structure is shown in Fig. 2. There is also an optics principle scheme of cone LED light source in Ref. 20. A dome light radiates indirect light at various angles. As the product is uniformly lit, a stable reliable inspection can be easily set up. To facilitate our decision-making process and provide unpolarized light over the whole product surface, we preferred diffuse dome lights that are very effective at lighting specular surface products and applying to defect detection with various and strong reflection surfaces.[20–22] In addition to improving system performance, it provided a clear surface information for SFS process and defect recognition.

2.2 *Shape from Shading*

When we mapped the 3-D world of our surface into a single 2-D image, the SFS deals with the recovery of the shape from shading variations. By using known or estimated scene informations, such as illumination, projection, or reflectance attributes, SFS methods are able to recover satisfying geometric details of the object.[23] It is a classic problem in computer vision with many potential applications.[24,25]

We start by giving a brief outline of the SFS problem and introducing the basic assumptions. Consider that $Z(x, y)$ is the surface expressed in terms of a function. The relationship between observed image intensity $I(x, y)$ and surface slopes $p = \frac{\partial Z}{\partial x}$, $q = \frac{\partial Z}{\partial y}$ can be expressed in an image irradiance equation as[26,27]

$$I(x, y) = \mathcal{R}(p, q, \mathfrak{l}, \vartheta, \rho), \tag{1}$$

where $\mathfrak{l}(\mathrm{i}1, \mathrm{i}2, \mathrm{i}3)$ is the illumination direction vector, $\vartheta(v1, v2, v3)$ is the vector from surface to the camera, and ρ is the albedo value. The orientation of surface can be completely defined by defining the normal to the surface at every point (x, y, z). The relationship between the surface slopes and normal can be expressed in terms of gradient and surface angles as in Eqs. (2) and (3), respectively

$$\eta(n1, n2, n3) = \frac{1}{\sqrt{1 + p^2 + q^2}}[-p, -q, 1]^T, \tag{2}$$

$$\eta(n1, n2, n3) = [(\sin\sigma n)(\cos\tau n), (\sin\sigma n)(\sin\tau n), (\cos\sigma n)]^T, \tag{3}$$

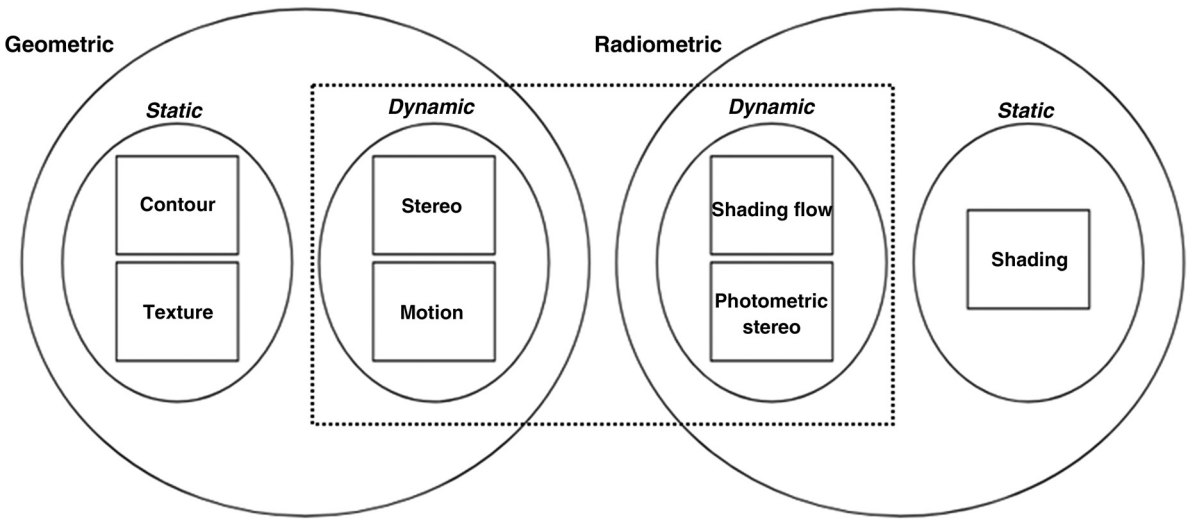

Fig. 1 Shape from X methods.[12]

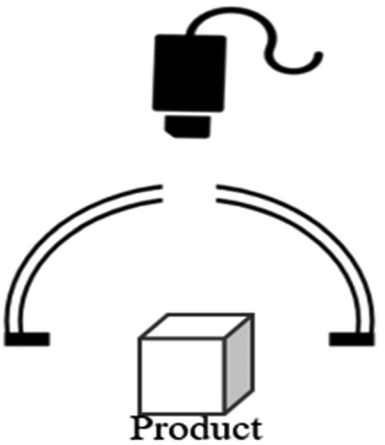

Fig. 2 Diffuse dome lighting structure.

where τn is the azimuth and σn is the zenith angle of the surface normal.

In SFS algorithms, one of the widely used models to represent surface reflectance with variations is the Lambertian model. In this model, the incident light on a surface is reflected equally in all directions. Reflected intensity is independent of the viewing direction and proportional to the cosine of the angle between the surface normal and light source direction. The below equation illustrates a Lambertian model image irradiance equation

$$I(x,y) = \rho \text{ł} \cdot \eta. \tag{4}$$

If the measured surface is not affected by highlights due to specular reflection, we can assume that the surface follows a Lambertian model.[15]

As can be easily understood from the above equations finding a unique solution to SFS is difficult. The method of obtaining shape information from one single image can be divided into four groups. Minimization approaches look for the solution by minimizing a cost energy function, propagation approaches propagate the shape information of points where the solution is known to the all unknown points over the whole image, linear approaches linearize the image irradiance equation, and local approaches approximate the surface based on a surface assumption (see Refs. 13 and 16). Let us take the issue of minimization briefly as it is in the center of this work. In minimization approaches, the solution of the SFS problem is obtained by minimizing an energy function over the entire image. The function to be optimized

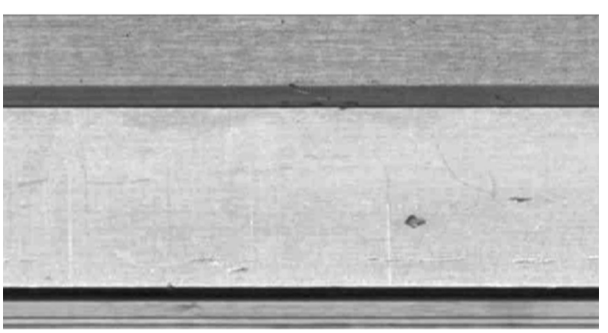

Fig. 3 Denoised image of the component's surface.

and the method of minimization should be considered in this approach. In studies of this scope, the cost function that has to be minimized is formed with different constraints, such as brightness, smoothness, integrability, and intensity gradient. Due to approximate solutions are typically local minima of the functional, a global optimization algorithm has to be used. In general, minimization approaches are more robust but need a longer CPU time than the others.[13]

2.2.1 *Shape from shading integrability*

Frankot and Chellappa project the nonintegrable gradient field onto a set of integrable slopes using the Fourier basis functions.[28] The approach is based on projecting the nonintegrable surface slope estimates onto the nearest-integrable surface slopes. They observed good results and the new extended algorithm showed improvements in both accuracy and efficiency over the original algorithm of Brooks and Horn (Ref. 29).[27] Let us consider Z_x and Z_y are the integrable surface slopes. Given a possibly noisy gradient field (p,q), we want to obtain $Z(x,y)$. With respect to given gradients, a square error function E can be written and it is also a map defined on every point (x,y) (see Ref. 28 for more information). So that finding optimal $Z(x,y)$ can be formulated as a minimization of this cost function

$$\text{cost(Z)} = \iint E(Z_x, Z_y, p, q)\mathrm{d}x\,\mathrm{d}y, \tag{5}$$

where

$$E(Z_x, Z_y, p, q) = (Z_x - p)^2 + (Z_y - q)^2. \tag{6}$$

The general approach of the Frankot and Chellappa algorithm assumes that the surface $Z(x,y)$ can be written as a linear combination of $\phi(x,y;\varpi)$ basis functions, where $\varpi = (\varpi_x, \varpi_y)$ is a 2-D index

$$Z(x,y) = \sum_{\varpi} C(\varpi)\phi(x,y;\varpi). \tag{7}$$

The above equation is the surface function and the below equation illustrates partial derivatives of the basis function in Eq. (7)

$$\phi_x(x,y;\varpi) = \frac{\partial \phi}{\partial x}(x,y;\varpi) \quad \phi_y(x,y;\varpi) = \frac{\partial \phi}{\partial y}(x,y;\varpi). \tag{8}$$

The orthogonality of basis functions greatly simplifies the minimization process. According to the first theorem of Frankot and Chellappa, Eq. (9) can be shown as the best coefficients in Eq. (7) that minimize the cost function with square error

$$\hat{\mathrm{C}}(\varpi) = \frac{P_x(\varpi)\hat{\mathrm{C}}_1(\varpi) + P_y(\varpi)\hat{\mathrm{C}}_2(\varpi)}{P_x(\varpi) + P_y(\varpi)}. \tag{9}$$

In the above equation

$$P_x(\varpi) = \iint |\phi_x(x,y;\varpi)|^2 \mathrm{d}x\,\mathrm{d}y$$

$$P_y(\varpi) = \iint |\phi_y(x,y;\varpi)|^2 \mathrm{d}x\,\mathrm{d}y. \tag{10}$$

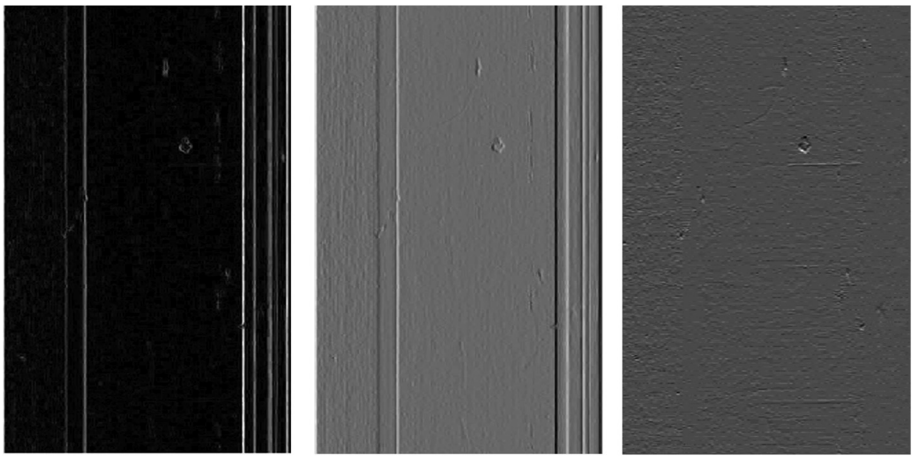

Fig. 4 (a) Gradient magnitude, (b) directional gradients along the *x*-axis, (c) and directional gradients along the *y*-axis.

This projection was fulfilled by finding the closest set of coefficients that satisfy integrability in the linear combination. Steps for recovering depth in our application are discussed in Sec. 3.

3 Recovering and Manipulating Depth Information

We first applied wavelet smoothing to remove noise from images obtained by the image acquisition system. Figure 3 shows the denoised image of the original component surface after the wavelet smoothing process.

Slope views in *x*- and *y*-directions are shown in Fig. 4. These two slope images in *x*- and *y*-direction are ideally suited for detecting defects with a specific orientation and shape deviations.

The choice of the basis function clearly affects the solution and because of its computational efficiency the discrete Fourier basis is frequently preferred. We used discrete Fourier basis in our equations. If we rewrite the $\phi(x, y; \varpi)$ function described in Sec. 2.2.1 as Fourier basis

$$\phi(x, y; \varpi) = e^{j2\pi\left(\frac{xu}{N}+\frac{yv}{M}\right)}, \tag{11}$$

where M and N are the dimensions of our image. Equation (12) is the partial derivatives of the basis function

$$\phi_x(x, y; \varpi) = \frac{j2\pi u}{N}\phi(x, y; \varpi)$$
$$\phi_y(x, y; \varpi) = \frac{j2\pi v}{M}\phi(x, y; \varpi). \tag{12}$$

Fig. 5 Combined side profile view of product surface. The boxes show some defects, such as cracks and scratches on the surface.

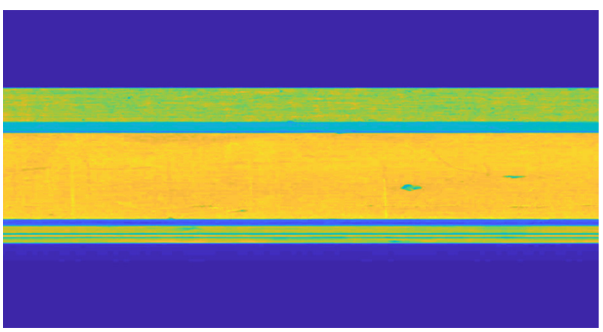

Fig. 6 Colored depth map of the surface.

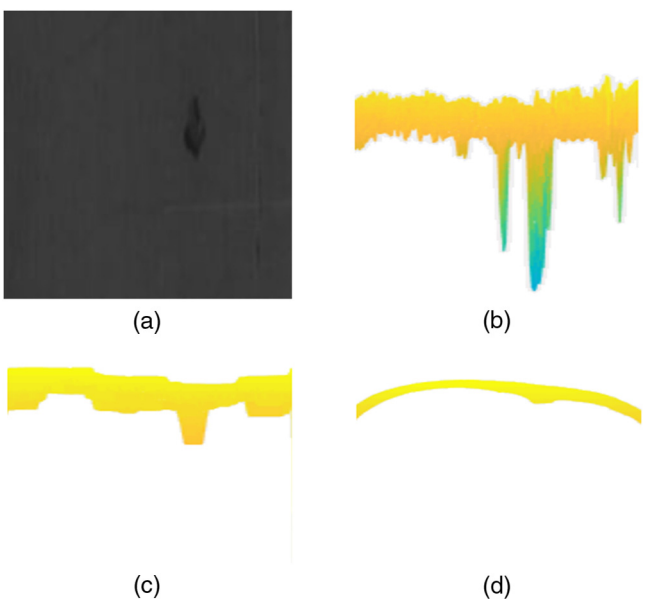

Fig. 7 Surface reconstruction using various algorithms: (a) top view of the surface defect, (b) the presented method, (c) Tsai–Shah algorithm, and (d) Pentland algorithm.

Simply, we took their powers for $P_x(\varpi)$ and $P_y(\varpi)$ (for detailed information about the algorithm see Ref. 27). Using discreate Fouirer transform (DFT) of p and q, the expansion coefficients $\hat{C}_1(\varpi)$ and $\hat{C}_2(\varpi)$ were calculated. Putting everything together and with respect to input p and q, the final output Z can be written as

$$Z = \mathcal{F}^{-1}\left\{-\frac{j}{2\pi}\cdot\frac{\frac{u}{N}\mathcal{F}\{p\}+\frac{v}{M}\mathcal{F}\{q\}}{(\frac{u}{N})^2+(\frac{v}{M})^2}\right\}, \tag{13}$$

where $\mathcal{F}\{\cdot\}$ and $\mathcal{F}^{-1}\{\cdot\}$ are the DFT and inverse DFT operations, respectively.

Based on the above-mentioned theory, a prototype inspection system has been implemented. Depending on the surface type, for example metal surfaces, features such as an illumination and reflection map should be well chosen. Note that the Lambertian model is not capable of describing specular reflections of shiny objects, such as metallic surfaces. Algorithms may perform differently related to surface material.

Table 1 General comparison of mentioned methods.

SFS method	Show details	Depth information	Wall-clock time (s)
Frankot and Chellappa	High	Good	1.72
Tsai–Shah (100 iterations)	Satisfactory	Moderate	5.94
Pentland	Low	Not promising results	0.1

4 Experimental Results

A defective product was chosen on purpose. In Fig. 5, the defective areas of the product surface are shown in blocks. Also a colored depth map is presented in Fig. 6.

Based on the image acquisition system, the size of the image of the product being examined may be too large, requiring a large memory for Fourier operations. We regionally analyzed the image. Detection performance of various algorithms was also discussed in this section. For comparison purposes, the results of some other SFS algorithms are shown in Fig. 7.

In Figs. 7(c) and 7(d), algorithms are based on the linearization of the reflectance map. Pentland's algorithm[30] uses the Fourier and inverse Fourier transform to obtain the depth map and takes direct linearization of the reflectance map in the surface gradient (p, q), while Tsai–Shah's algorithm[31] uses the Newton method and linearized the reflectance map in terms of the depth Z using Taylor series expansion directly. Tsai–Shah offers an iterative solution.

As can be seen from the results in Fig. 7, the proposed approach provides a much more detailed and deep solution than the other two algorithms. When the depth calculation times of the algorithms were compared after 800×600 images were taken, the required wall-clock time for (b) the proposed method is 1.72 s, for (c) Tsai–Shah with 100 iterations (not satisfactory results in lower iterations) is 5.94 s and for (d) Pentland is 0.1 s. The proposed algorithm results in a much deeper depth map, while the (c) algorithm calculates moderate depth and (d) has a shallow depth. A general comparison of the above-mentioned methods is shown in Table 1.

Minimization approaches can be preferred in applications where details are important. However, in situations where rapid results and decision-making are required, the use of other SFS methods can be considered. There are literature

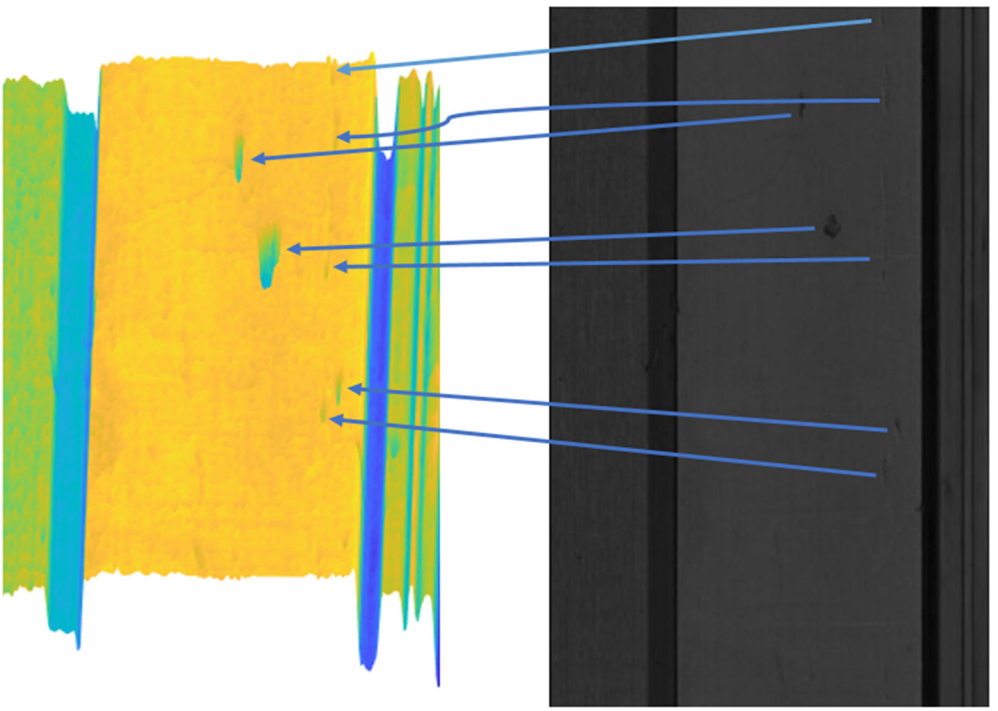

Fig. 8 Overall reconstruction result of the surface.

studies based on their estimates of albedo and light location values in unknown cases. Using a known light source orientation and nonconstant albedo values can produce stronger results. For a more effective solution, new algorithmic solutions integrated with other robust shape recovery approaches can be produced. The clarity and quality of the taken image will affect its performance in the inspection algorithm.

In this work, we focused on one of the minimization approaches of SFS algorithms. Figure 8 shows the overall result of the reconstruction for our system. The defect regions are clearly visible on the visualization of the depth map. The average length of the scratches and cracks detected here varies between 0.5- and 2.5-mm length. Our classification algorithm interprets the values of the incoming pixel and neighboring pixels and decides whether the defect is a scratch, crack, or hole. As a result of all this, it can be decided that the product is usable or defective.

5 Conclusion

A minimization-based SFS algorithm is implemented with the purpose of a surface inspection system for industrial components. Since some parts perform extremely important functions and of very delicate quality, as in the car industry, all the components of such a system must be tested in a very detailed method. SFS is a robust technology for detecting the finest defects even on challenging surfaces. In experiments with metallic surfaces, it is demonstrated that the presented approach works for tiny defects. In our future work, we can focus on developing more reliable, faster and timely to decide algorithms by integrating the features of shape recovery methods that remove each other's disadvantages, and we intend to strengthen minimization approaches with the help of recently developed optimization methods.

Acknowledgments

This study is partially supported by the Scientific and Technological Research Council of Turkey (TUBITAK) (Project No. 5160018), Sakarya University and Sakarya University Scientific Research Projects Unit.

References

1. J. Molleda et al., "An improved 3D imaging system for dimensional quality inspection of rolled products in the metal industry," *Comput. Ind.* **64**(9), 1186–1200 (2013).
2. T. S. Newman and A. K. Jain, "A survey of automated visual inspection," *Comput. Vision Image Understanding* **61**(2), 231–262 (1995).
3. R. S. Deshmukh et al., "Comparison analysis for efficient defect detection algorithm for gray level digital images using median filters Gabor filter and ICA," *Int. J. Adv. Res. Comput. Sci. Software Eng.* **2**(1), 34–38 (2012).
4. P. P. Jonker et al., "Pattern recognition for metal defect detection," *Steel Grips* **1**(1), 20–23 (2003).
5. S. H. Choi et al., "Real-time defects detection algorithm for high-speed steel bar in coil," in *Proc. of World Academy of Science, Engineering and Technology*, Vol. **21**, pp. 1307–6884 (2007).
6. J. L. Rahejaa et al., "Fabric defect detection based on GLCM and Gabor filter: a comparison," *Optik* **124**, 6469–6474 (2013).
7. Z. Xue-wu et al., "A vision inspection system for the surface defects of strongly reflected metal based on multi-class SVM," *Expert Syst. Appl.* **38**(5), 5930–5939 (2011).
8. F. Pernkopf, "Detection of surface defects on raw steel blocks using Bayesian network classifiers," *Pattern Anal. Appl.* **7**(3), 333–342 (2004).
9. F. Pernkopf, "3D surface acquisition and reconstruction for inspection of raw steel products," *Comput. Ind.* **56**(8–9), 876–885 (2005).
10. D. Quanying et al., "Inspection of weld shape based on the shape from shading," *Int. J. Adv. Manuf. Technol.* **27**(7–8), 667–671 (2006).
11. J. E. Cryer et al., "Combining shape from shading and stereo using human visual model," UCF Technical Report CS-TR-92-25, University of Central Florida, Florida (1992).
12. S. Negahdaripour, "Revised definition of optical flow: integration of radiometric and geometric cues for dynamic scene analysis," *IEEE Trans. Pattern Anal. Mach. Intell.* **20**(9), 961–979 (1998).
13. R. Zhanget et al., "Shape-from-shading: a survey," *IEEE Trans. Pattern Anal. Mach. Intell.* **21**(8), 690–706 (1999).
14. P. Bergström et al., "Automatic in-line inspection of shape based on photogrammetry," in *7th Int. Swedish Production Symp.*, Lund, Sweden, pp. 1–9 (2016).
15. D. Kang et al., "Development of an inspection system for planar steel surface using multispectral photometric stereo," *Opt. Eng.* **52**(3), 039701 (2013).
16. J. D. Durou et al., "Numerical methods for shape-from-shading: a new survey with benchmarks," *Comput. Vision Image Understanding* **109**(1), 22–43 (2008).
17. Y. Xu et al., "Wavelet transform domain filters: a spatially selective noise filtration technique," *IEEE Trans. Image Process.* **3**(6), 747–758 (1994).
18. J. B. Weaver et al., "Filtering noise from images with wavelet transforms," *Magn. Reson. Med.* **21**(2), 288–295 (1991).
19. J. Lu et al., "Noise reduction by constrained reconstructions in the wavelet transform domain," in *Proc. of the Seventh Workshop on Multidimensional Signal Processing*, Lake Placid, New York (1991).
20. B. Liu et al., "Automatic detection technology of surface defects on plastic products based on machine vision," in *Int. Conf. on Mechanic Automation and Control Engineering*, Wuhan, China (2010).
21. L. Li et al., "Improved illumination for vision-based defect inspection of highly reflective metal surface," *Chin. Opt. Lett.* **11**(2), 021102 (2013).
22. D. Martin, "*A Practical Guide to Machine Vision Lighting*," Midwest Sales and Support Manager, VT: Advanced Illumination, Rochester (2007).
23. L. Jiang et al., "3D face reconstruction with geometry details from a single image," *CoRR*, abs/1702.05619 (2017).
24. M. Breuß et al., "Efficient numerical techniques for perspective shape from shading," in *Proc. of Algoritmy*, Podbanske, Slovakia (2009).
25. M. Breuß et al., "Numerical algorithms for perspective shape from shading," *Kybernetika* **46**(2), 207–225 (2010).
26. B. Horn, "Obtaining shape from shading information," in *The Psychology of Computer Vision*, P. Winston, Ed., pp. 115–155, McGraw-Hill, New York (1975).
27. R. T. Frankot and R. Chellappa, "A method for enforcing integrability in shape from shading algorithms," *IEEE Trans. Pattern Anal. Mach. Intell.* **10**(4), 439–451 (1988).
28. A. Agrawal et al., "What is the range of surface reconstructions from a gradient field?" in *Proc. of the 9th European Conf. on Computer Vision (ECCV)* (2006).
29. M. J. Brooks and B. K. P. Horn, "Shape and source from shading," in *Proc. Int. Joint Conf. Artificial Intelligence*, Los Angeles, California (1985).
30. A. Pentland, "Shape information from shading: a theory about human perception," in *Second Int. Conf. on Computer Vision*, pp. 404–413 (1988).
31. P. Tsai and M. Shah, "Shape from shading using linear approximation," *Image Vision Comput.* **12**(8), 487–498 (1994).

Muhammed Kotan received his BS degree in computer engineering and MS degree in computer and information engineering from Sakarya University, Turkey, in 2011 and 2014, respectively. He is currently pursuing his PhD and working in the Information Systems Engineering Department, Sakarya University. His current research interests include image processing, computer vision, and virtual reality.

Cemil Öz received his BS degree in electronics and communication engineering from Yıldız Technical University in 1989 and his MS degree in electronics and computer education from Marmara University, Istanbul, in 1993. During his MS studies, he worked as a lecturer at Istanbul Technical University. In 1994, he began his PhD study in electronics engineering at Sakarya University. He completed his PhD in 1998. He worked as a research fellow at the University of Missouri-Rolla, Missouri, USA. He has been working as a professor at the Computer and Information Sciences Faculty, Department of Computer Engineering, Sakarya University. His research interests include robotics, vision, artificial intelligence, virtual reality, and pattern recognition.